Geophysical Research Letters

RESEARCH LETTER
10.1029/2020GL091156

The Effect of Aerosols on Fog Lifetime: Observational Evidence and Model Simulations

Shuqi Yan[1,2,3,4], Bin Zhu[1,2,3,4], Tong Zhu[5], Chune Shi[6], Duanyang Liu[7,8], Hanqing Kang[1,2,3,4], Wen Lu[1,2,3,4], and Chunsong Lu[1,2,3,4]

[1]Collaborative Innovation Center on Forecast and Evaluation of Meteorological Disasters, Nanjing University of Information Science & Technology, Nanjing, China, [2]Key Laboratory for Aerosol-Cloud-Precipitation of China Meteorological Administration, Nanjing University of Information Science & Technology, Nanjing, China, [3]Key Laboratory of Meteorological Disaster, Ministry of Education (KLME), Nanjing University of Information Science & Technology, Nanjing, China, [4]Special Test Field of National Integrated Meteorological Observation, Nanjing University of Information Science & Technology, Nanjing, China, [5]IMSG at NOAA, NESDIS/STAR, 5830 University Research Ct., College Park, MD, USA, [6]Key Laboratory of Atmospheric Sciences and Satellite Remote Sensing of Anhui Province, Anhui Institute of Meteorological Sciences, Hefei, China, [7]Key Laboratory of Transportation Meteorology, China Meteorological Administration, Nanjing, China,[8]Nanjing Joint Institute for Atmospheric Sciences, Nanjing, China

Key Points:

- Fog frequency in East China is decreasing, and fog duration is increasing
- The increase in fog duration is mainly caused by aerosols
- Aerosol–cloud interaction plays a more important role in increasing fog duration than aerosol–radiation interaction

Supporting Information:

- Supporting Information S1

Correspondence to:
B. Zhu,
binzhu@nuist.edu.cn

Citation:
Yan, S., Zhu, B., Zhu, T., Shi, C., Liu, D., Kang, H., et al. (2021). The effect of Aerosols on Fog lifetime: Observational evidence and model simulations. *Geophysical Research Letters*, *48*, e2020GL61803. https://doi.org/10.1029/2020GL091156

Received 15 OCT 2020
Accepted 22 DEC 2020

Abstract The aerosol–cloud interaction (ACI) and aerosol–radiation interaction (ARI) have notable influences on clouds, but their effects on fog are rarely analyzed before. Previous studies indicate that fog frequency in East China has been decreasing, and we further reveal that fog duration increases during 1960–2010. We hypothesize that this trend is related to the increase of aerosol pollution and perform WRF-Chem simulations to study the ARI and ACI effects. Results show that ACI significantly advances fog formation, delays fog dissipation, and increases fog duration by about 1 h in a case study, while ARI has negligible effect. The more but smaller fog droplets produced in polluted conditions significantly inhibit droplet sedimentation and reduce solar radiation, therefore provide favorable conditions for the duration of fog. Under extremely polluted conditions, ACI effect also far overweighs ARI effect. To shorten the duration of dense fog, our findings suggest the necessity for mitigating emissions.

Plain Language Summary Aerosols, the suspensions of solid or liquid particles in the air, affect clouds through aerosol–cloud interaction (ACI) and aerosol–radiation interaction (ARI). The ARI refers to that aerosols affect the meteorological conditions in clouds by scattering and absorbing radiation. The ACI refers to that clouds form on aerosols if aerosols absorb sufficient water vapor. Fog is a kind of near-surface cloud. The ARI and ACI could have both notable influences on fog, but their effects are rarely analyzed before. Previous studies indicate that fog frequency in East China has been decreasing, and in this study we further reveal that fog duration increases during 1960–2010. We hypothesize that this trend is related to the increase of aerosol pollution and perform numerical simulations to study the ARI and ACI effects. Results show that ACI significantly advances fog formation, delays fog dissipation, and increases fog duration by about 1 h in the case study, while ARI has negligible effect. The ACI can significantly inhibit fog droplet sedimentation and reduce solar radiation, therefore provide favorable conditions for the duration of fog. Our findings suggest that reducing emissions could shorten fog duration and mitigate the hazards of fog.

1. Introduction

The intensive anthropogenic emissions and high aerosol loading in East China have profound impacts on clouds and precipitations (Gu et al., 2006; J. Guo et al., 2019; Z. Li et al., 2016; Wu et al., 2016). The complex interaction between aerosols and clouds has attracted worldwide attention since the late 1980s (Z. Li et al., 2019). Aerosols affect clouds through aerosol–radiation interactions (ARIs) and aerosol–cloud interactions (ACIs) (Fan et al., 2016; IPCC, 2013). Many studies have revealed that the impacts of ARI and ACI on clouds are remarkable and diverse, contingent on cloud types, aerosol properties, and meteorological conditions (e.g., Gu et al., 2017; Koren et al., 2008; Z. Li et al., 2011; Rosenfeld et al., 2008). Fog can be viewed as a kind of cloud that resides near the surface (Zhu & Guo, 2016). The high concentration and notable diurnal variation of surface aerosols could complicate the effect on fog, so it is an interesting topic to study the impacts of the ARI and ACI effects on fog.

The ARI could remarkably influence planetary boundary layer (PBL) thermodynamic structure by perturbing radiation transfer, which was named as aerosol dome effect by A. J. Ding et al. (2016) and reviewed by Z. Li et al. (2017). Aerosols can block the solar radiation reaching the ground, reduce surface heat flux, and cool the near-surface air (A. J. Ding et al., 2013; Z. Li et al., 2007); black carbon especially can effectively trap more solar radiation and heat the upper PBL (Bond et al., 2013). Such surface cooling and upper-level heating effects stabilize stratification and weaken turbulent mixing, which decreases PBL height and leads to the accumulation of moisture and pollutants (Huang et al., 2020). The increased humidity and aerosols can further enhance pollution and suppress PBL by a positive feedback (Tie et al., 2017). The ARI may also alter the formation and dissipation conditions of fog through similar processes. Bott (1991) found that the abundant absorbing aerosols in urban areas can delay fog dissipation by reducing downwelling solar radiation and decreasing near-surface temperature.

The ACI is one of the most challenging and complicated processes in understanding the mystery of clouds. Under saturated condition and constant liquid water content (LWC), additional aerosols produce more but smaller droplets, leading to larger cloud albedo and optical depth (Twomey, 1977). As a result, fog in polluted conditions can block more solar radiation reaching the ground and inhibit dissipation. Additionally, the decreased droplet size slows down autoconversion and sedimentation rates, which can increase the residence time of cloud water (Albrecht, 1989) and favor the maintenance of fog. Many modeling studies have confirmed that increasing aerosols could promote fog, with higher LWC, more fog droplets, higher liquid water path (LWP), and longer persistence (e.g., Jia et al., 2018; Maalick et al., 2016; Stolaki et al., 2015; Yan et al., 2020).

Long-term variation of fog frequency and fog lifetime are both important climatic characteristics of fog. Previous studies have revealed that long-term fog frequency in East China is decreasing (e.g., Y. Ding & Liu, 2014; Fu et al., 2014; T. Guo et al., ; Yan et al., 2019). However, few studies have revealed the trend in fog lifetime and investigated the effects of aerosols on fog lifetime (features of formation, development, dissipation, and duration). In this study, we first reveal the long-term variation in fog duration and its relation with the increase of aerosol pollution. Since ARI and ACI effects cannot be separated in observational data, we further disentangle and quantify these two factors by online-coupled WRF-Chem simulations. Investigating the individual contributions of ARI and ACI will help us to better understand the evolution of fog events, enrich the knowledge of ACIs, and provide clues to mitigate the hazard of fog weather.

2. Data and Model Configuration

A long-term (1960–2010) manually recorded fog data are used to analyze the variation of fog duration (Deng et al., 2015; Shi et al., 2008). It includes the formation and dissipation times of each fog event with accuracy in minutes. The same data set is used in this study, which includes 9 stations in Anhui Province and 10 stations in Jiangsu Province, China (Figure 1 and Table S1). In our analysis, two consecutive fog events are recognized as one event if the time difference between current fog formation and previous fog dissipation is less than 1 h (Shi et al., 2008). In the second part, the modeling study, a 3-hourly temperature, dew point, and visibility data from the Meteorological Information Comprehensive Analysis and Process System (Y. Li et al., 2010) are used to evaluate model performance of meteorological fields and fog characteristics. The hourly $PM_{2.5}$ concentration data from China National Environmental Monitoring Center are also used to evaluate model performance of $PM_{2.5}$.

To investigate the mechanism of how ARI and ACI affect fog duration, the WRF-Chem (V3.9.1.1), an online-coupled model, is used to simulate a long-lasting fog event occurred in East China from December 31, 2016 to January 4, 2017. This model is widely used to assess aerosol direct (or ARI) and indirect effects (or ACI). A brief description of aerosol processes and aerosol effects (AEs) is in Text S1, and the detailed descriptions can also be found in Chapman et al. (2009) and Fast et al. (2006). One domain is set with the size of 139 × 145 grids and 9-km resolution (Figure 1), which covers the entire region of this fog event. The vertical levels are refined to 42 levels and nine of them are under 100 m. The grid analysis nudging and observation nudging are turned on (Borge et al., 2008), which can greatly improve the model performance

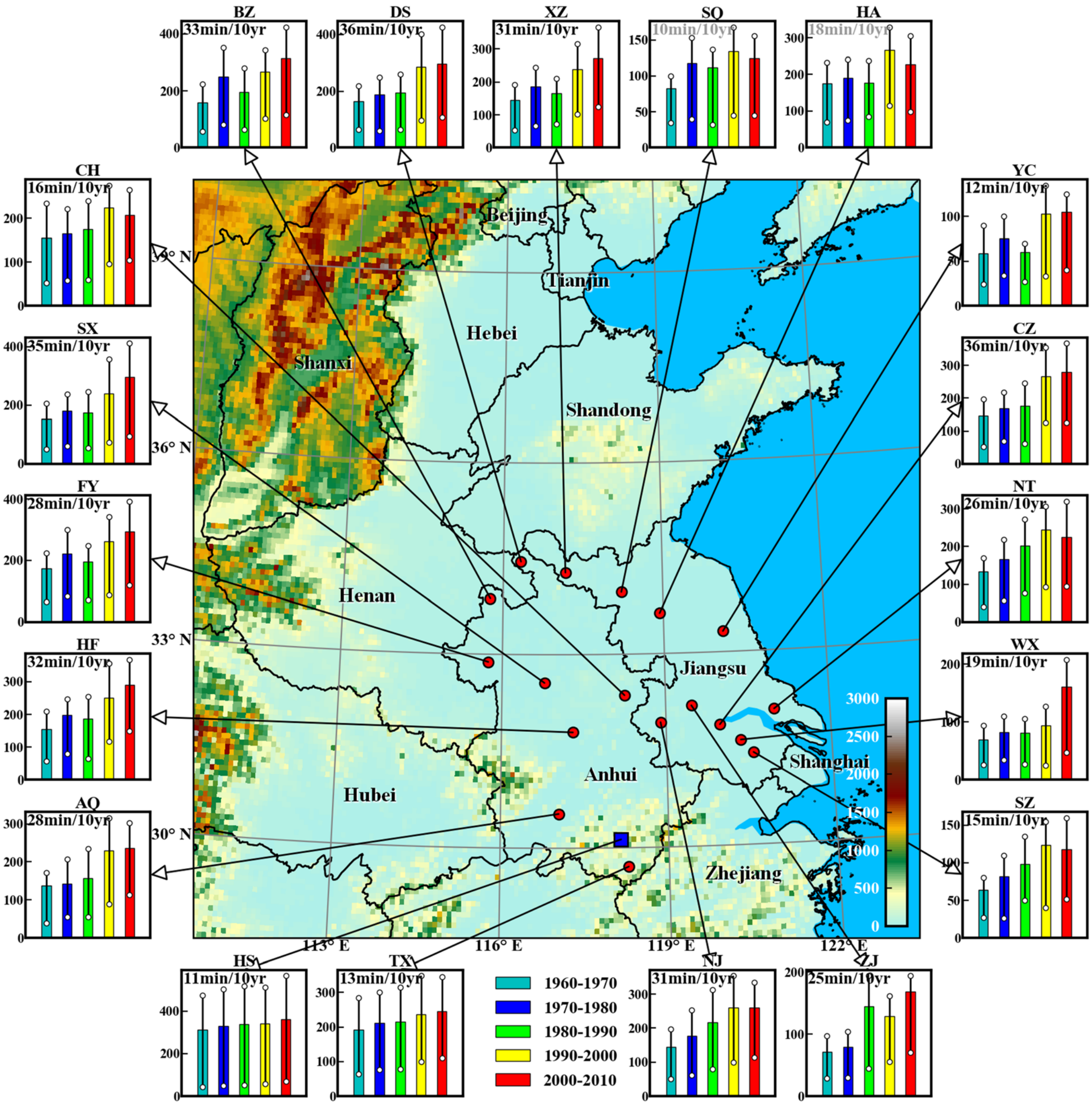

Figure 1. The model domain with the locations of 19 stations (center panel). The blue square is Huangshan, a background station. The surrounding panels are the decadal variation of fog duration (min) with error bars representing the 25% and 75% percentile. The upper left texts are the linear trends of fog duration with the meanings explained in Section 3, and the insignificant ($\alpha = 0.05$) trends are colored by gray. The province names are marked.

of fog. Detailed physical and chemical schemes are listed in Table S2. The input of meteorological field is ECMWF (0.125°) reanalysis, and the anthropogenic inventory is Multiresolution Emission Inventory for China (MEIC) (M. Li et al., 2014). No biomass burning, sea salt, or dust emission are used, because their emissions or concentrations are relatively low during the simulation period. The simulation starts at 08:00 LST on December 28, 2016 and ends at 08:00 LST on January 4, 2017, and the first 3 days is used as the spin-up period. All the times in this study are local standard time (LST or UTC + 8).

To isolate ARI and ACI from total AE, three sensitive experiments, A0, A1DE0, and A1 are conducted (Table S3), following the design by Fan et al. (2015) and Zhong et al. (2015). A1 and A1DE0 represent the current polluted condition that uses the original MEIC inventory. A1 is the base condition that includes full AE, while A1DE0 excludes the ARI effect in A1 by setting aerosol optical depth (AOD) as zero in radiation transfer schemes. A0 represents the clean condition in which the emission intensity is multiplied by 0.05 (Jia et al., 2018), and the ARI effect in A0 can be safely ignored (Fan et al., 2015). Therefore, the effects of ARI, ACI, and AE can be quantified by the differences of A1 − A1DE0, A1DE0 − A0, and A1 − A0, respectively. In this study, the simulated fog is defined by the LWC > 0.01 g/kg within the PBL (Kunkel, 1984), equivalent to the horizontal visibility less than about 1.0 km. Fog over ocean or water body are not considered in the study.

3. Aerosols Increase Fog Duration: Observational Evidence

A few studies have revealed the decadal variation of fog duration (Deng et al., 2015; Shi et al., 2008), because the temporal resolution of long-term observational data is normally 6 h, which cannot accurately identify the starting and ending time of fog events. Fortunately, the high temporal resolution of the manually recorded data in Section 2 allows the study of fog duration. Our previous study found that fog frequency in East China was decreasing (Yan et al., 2019), and in this study we find that fog duration increases significantly ($\alpha = 0.05$) at 17 out of 19 stations during 1960–2010 (Figure 1). For example, at HS station, the 50-year-average fog duration is 336 min, and the increasing trend is 11 min (3.3%) every 10 years Deng et al. (2015) and Shi et al. (2008) also reported the similar increasing trends in Anhui Province. The change in fog duration is affected by climate change, urbanization, and aerosol pollution (Yan et al., 2019). To exclude the role of climate change, we compare background and nonbackground stations. HS is selected as the background station in East China (J. Gao et al., 2017). Since it is located at a relatively high altitude (1,836 m), HS can represent the regional climate background and clean conditions.

The increased fog duration at HS may be resulted from climate change and increasing aerosols in regional background. Both HS and other stations in East China show decreasing trends in wind speed that favors fog maintenance (Niu et al., 2010; J. Zhang et al., 2017), and the humidity-corrected visibility at HS decreases generally from 1960 to 2010 (Jiang et al., 2014). At other 18 stations where air pollution is more serious, the increase in fog duration (on average 25 min/10 years, 13.8%) is more obvious than that at HS (11 min/10 years, 3.3%). Among the 18 stations, two provincial capitals, NJ and HF are picked out to further support the AE on fog duration. NJ and HF are usually more polluted than other stations, and the increase in fog duration is even stronger (32 min/10 years, 14.9%). Based on previous studies, we speculate that there is a strong correlation between the increase of aerosols and the increase of fog duration and hypothesize that ARI and ACI both promote fog duration. In observational data, the relative contributions of ARI and ACI cannot be quantitatively separated, so we will perform the investigation by using the WRF-Chem simulations in the following section.

4. The Respective Effects of ARI and ACI: Model Simulations

An extreme fog event lasted from December 31, 2016 to January 4, 2017 in East China (N. Zhang & Ma, 2017), covering vast areas of Hebei, Henan, Shandong, Anhui, Jiangsu, Hubei provinces. Temperature and dew point are two vital meteorological factors related to fog. By evaluating the performance of control experiment (A1), it is found that the root mean square errors for temperature and dew point are 1.7 K and 1.2 K, respectively (Figures S1(b) and S1(d)). The time series of domain-averaged temperature and dew point are well reproduced by the simulation, and the correlation coefficients of them are both 0.98 (Figures S1(a) and S1(c)). The A1 experiment also simulates the variation of $PM_{2.5}$ reasonably well, with the correlation coefficient of 0.77 (Figure S2). Figures 2(a)–2(d) evaluate the performance of simulated fog spatial distribution. At 08:00 on January 1, the simulation underestimates the fog in northern Jiangsu and western Shandong. At 08:00 on January 2 and 3, the simulated fog area agrees well with the observation. At 08:00 on January 4, the simulation overestimates the fog in Anhui. In general, the A1 experiment (control run) well captures the temperature, water vapor fields, and the fog spatial distributions.

By comparing the three experiments, we first examine the general effects of ARI and ACI in terms of domain-averaged fog features (Figures 2(e)–2(h)). As shown in Figures 2(e) and 2(f), there are four fog events in this case study. In the average of the four subevents, the fog duration of control experiment (A1) is 6.16 h. The ARI slightly influences LWC, fog area, and fog duration, and the change in fog duration is only 3 min. On the other hand, ACI substantially increases LWC, expands fog area, and extends fog duration by

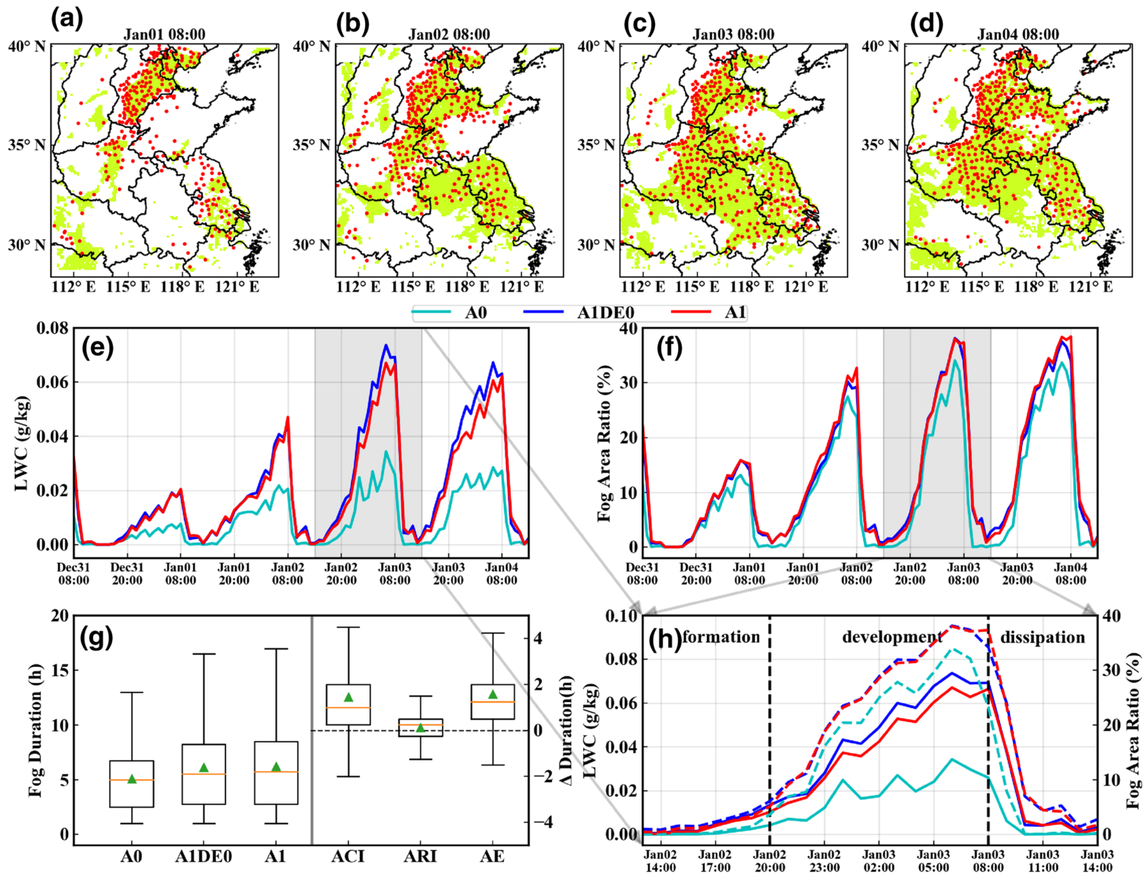

Figure 2. (a–d) The distribution of observed and simulated fog. The observed fog (red points) is represented by the MICAPS stations with horizontal visibility <1.0 km and relative humidity >90%. The simulated fog (shaded color) is represented by LWC > 0.01 g/kg in control experiment. (e, f) The domain-averaged time series of LWC and fog area ratio for experiments A0, A1, and A1DE0. (g) Left part, four-event-mean fog durations of the three experiments, and right part, the change of fog duration induced by ACI, ARI, and AE with min/max tick, median (orange line), and average (green triangle). (h) The zoom-in time series of LWC (solid) and fog area ratio (dashed) for the third event that will be analyzed in the next. MICAPS, Meteorological Information Comprehensive Analysis and Process System; LWC, liquid water content; ACI, aerosol–cloud interaction; ARI, aerosol–radiation interaction; AE, aerosol effect.

66 min. The total AE causes a 69 min (23%) increase in fog duration, which is similar to the value (57 min; 14%) revealed by Jia et al. (2018). The impact of aerosols on fog or cloud depends on aerosol concentration and water vapor content (Chen et al., 2012). To examine ACI and ARI effects under different moisture and pollution conditions, Table S4 compares ACI and ARI-induced change in fog duration over urban, rural, polluted, and clean regions. It is found that fog durations in both urban and rural regions are significantly increased owing to ACI. The ACI-induced increase in fog duration in polluted regions (90 min) is twice more than that in clean regions (43 min). In contrast, the influence of ARI on fog duration is limited to 9 min (insignificant under $\alpha = 0.05$). Therefore, the promoting effect of aerosols on fog duration is mainly contributed by ACI.

To explore the mechanisms of ARI and ACI, we analyze the third fog event (13:00 January 2 to 14:00 January 3) in more detail, because this event is well simulated and has the highest intensity. According to the temporal variation (Figure 2(h)), we roughly divide this event into formation stage (13:00–21:00), developing stage (21:00–08:00), and dissipation stage (08:00–14:00) in the following analysis.

Figure 3 shows the impact of aerosols on the coverage of fog and time series of downwelling solar radiation, temperature, and relative humidity (RH) for the three experiments during the formation stage. At 13:00 LST, the previous fog event nearly dissipates entirely in all three experiments. By 20:00 LST, fog develops in all the experiments, while fog areas are larger under polluted conditions (A1DE0 and A1). Therefore, we can conclude that ACI advances fog formation, while ARI has nonobvious effect. To explain the ACI effect, we perform some detail diagnoses within the area as shown in the black box of Figure 3. At 13:00 LST, the

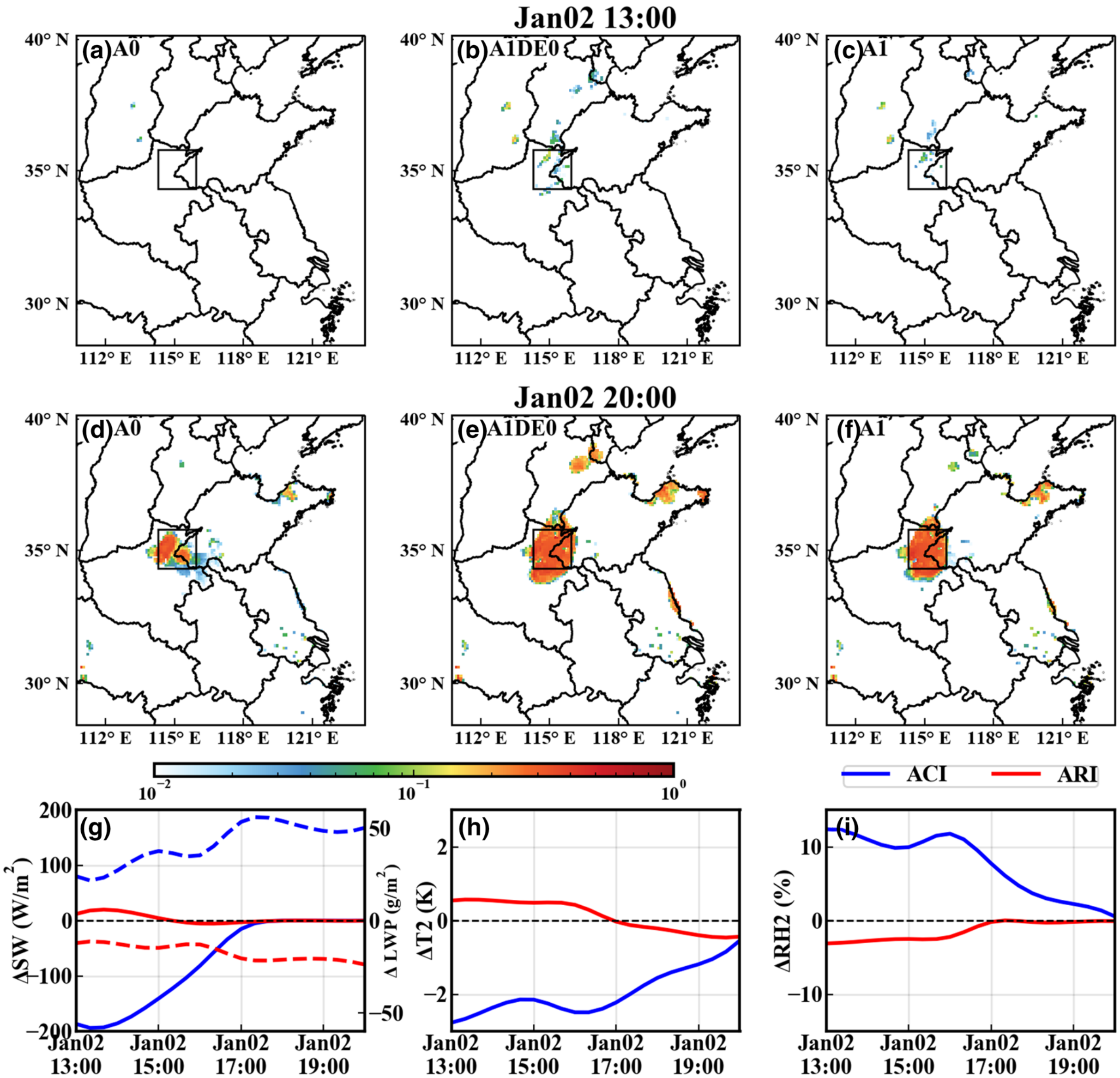

Figure 3. Fog distributions for experiments A0, A1DE0, and A1 at two typical times during formation stage (a–f). The shaded color represents LWC. (g–i) The time series of the ARI and ACI-induced changes in surface downwelling solar radiation (SW), LWP (dashed lines), 2 m air temperature (T2), and 2 m relative humidity (RH2) within the black box in (a)–(f). LWC, liquid water content; ARI, aerosol–radiation interaction; ACI, aerosol–cloud interaction; LWP, liquid water path.

upper-level fog in A1DE0 does not disappear (up to ∼160 m), leading to an increase in LWP and a significant reduction in solar radiation (185 W/m^2) at the surface (Figure 3(g)). Therefore, ACI results in lower temperature (maximum 2.8 K reduction) and higher RH (maximum 12 % increase) (Figures 3(h) and 3(i)), which promote aerosol activation and fog formation. However, the maximum changes in solar radiation (+20 W/m^2), temperature (+0.5 K), and RH (-3.5%) induced by ARI are not comparable to that by ACI. It indicates that the ARI effect is outweighed by ACI effect when fog is present. The change in solar radiation by ARI is positive, which may be because that the LWP in A1 experiment is lower than that in A1DE0 (Figure 3(g)).

During the development stage, the differences of fog characteristics among the three experiments are mainly reflected by LWC (Figure 2(h)). The LWC differences can be explained by the comparisons among fog microphysical parameters (Figure S3). Overall, the ACI effect is dominant over the ARI effect. In polluted conditions (A1 and A1DE0), the cloud condensation nuclei (CCN) is approximately 1 order of magnitude higher than that in clean condition (A0). The abundant CCN promotes activation under the saturation envi-

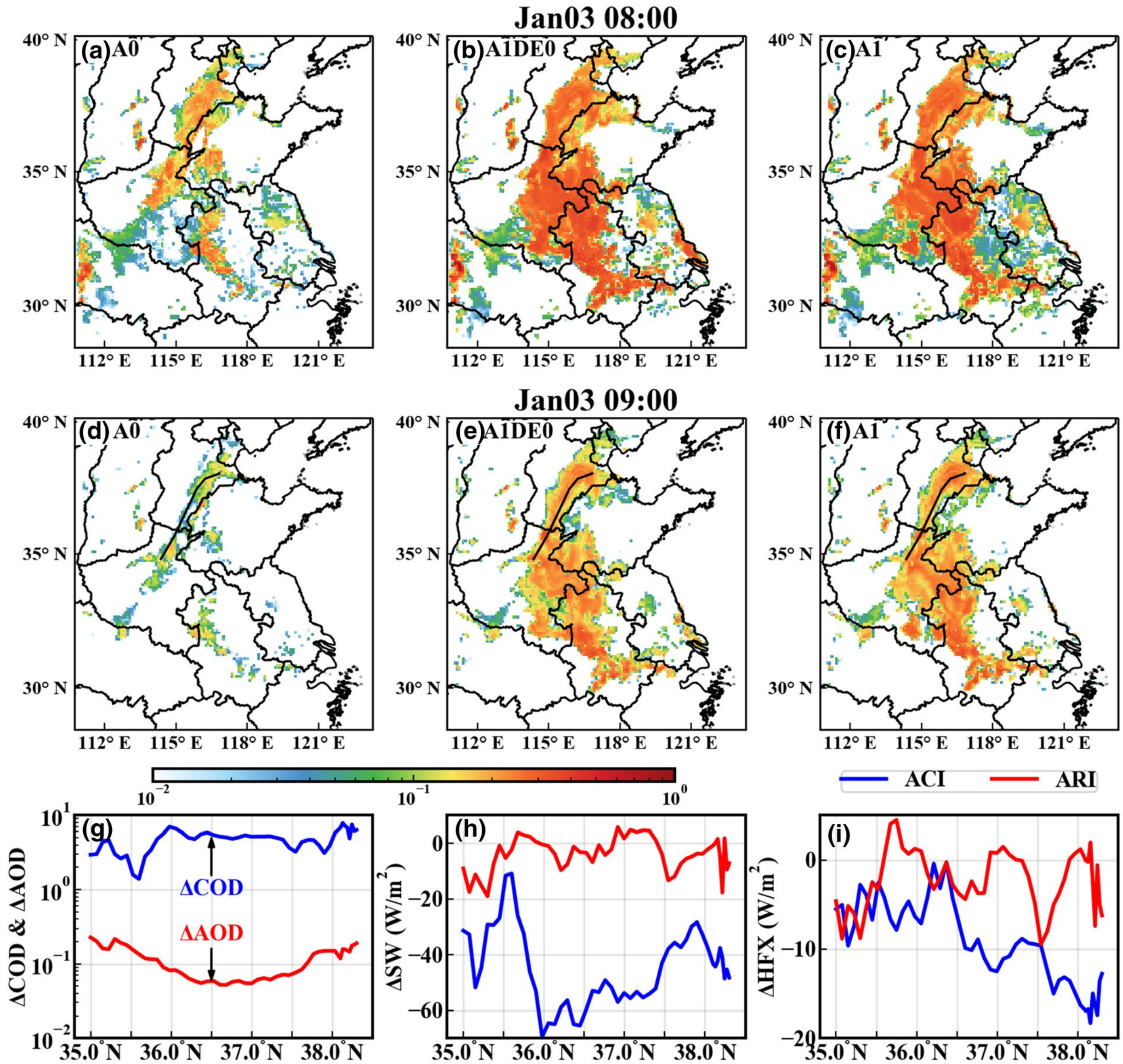

Figure 4. Same as Figure 3, but for dissipation stage (a–f). (g) The latitudinal distribution of the change in COD (AOD) induced by ACI (ARI) at the black crossing line in (d)–(f). (h, i) Same as (g), but for surface downwelling solar radiation (ΔSW) and surface heat flux (ΔHFX), respectively. COD, cloud optical depth; AOD, aerosol optical depth; ACI, aerosol–cloud interaction; ARI, aerosol–radiation interaction.

ronment and increases fog droplets from less than 50 cm^{-3} to higher than 100 cm^{-3}. As a result, the increased water vapor competition in condensation growth causes a smaller droplet radius and decreases sedimentation velocity. It can increase the residue time of fog droplets, thus promote fog maintenance and lead to a higher LWC. Promoting effects of ACI on fog under higher aerosol concentration have been revealed by many studies (e.g., Jia et al., 2018; Maalick et al., 2016; Stolaki et al., 2015). Before sunrise (08:00), the microphysical effects of ACI can also prolong fog duration and enlarge fog area (Figures 2(h) and Figure 4(a) vs. 4(b)). After sunrise, the larger cloud optical depth (COD) induced by ACI can delay fog dissipation by substantially reducing solar radiation, which will be discussed next.

Figure 4 shows the impact of aerosols on the coverage of fog during the dissipation stage. At 08:00 LST, the clean condition (A0 experiment) underestimates fog area, while the A1DE0 experiment with ACI effect could rightly simulate the fog area, which increases the hit rate (Zhou & Du, 2010) from 41% (A0) to 63% (A1DE0). At 09:00 LST, fog dissipates fast in A0 but slowly in A1 and A1DE0. The delayed dissipation due to ACI can be explained by the influences of AOD and COD on solar radiation, because solar radiative heating lies at the root of fog dissipation. Under polluted conditions, ACI and ARI can yield larger COD and AOD, respectively. Since fog droplets have much stronger extinction ability than aerosols, the increase in COD is approximately 1 order of magnitude higher than that in AOD (Figure 4(g)). Accordingly, the larger COD can block more solar radiation reaching the ground. The ACI (ARI) causes a reduction of 20–60 (0–20) W/m^2 in solar radiation and a 5–20 (0–10) W/m^2 reduction in sensible heat flux (Figures 4(h) and 4(i)). Therefore, it is ACI that significantly blocks solar radiation and decreases sensible heat flux, leading to the delayed dissipation and longer lifetime of fog. Maalick et al. (2016) and Stolaki et al. (2015) also found that ACI can notably prevent fog dissipation.

Previous studies demonstrate that ARI is the decisive factor in affecting PBL structure and air quality under severe pollution episodes (e.g., Y. Gao et al., 2015; Huang et al., 2020). To evaluate if ACI effect on fog also overweighs ARI effect under a more polluted condition, we conduct two extra experiments, A3 and A3DE0, which represent the extremely polluted condition (Table S3). The average fog duration in A0, A3DE0, and A3 are 5.10, 6.51, and 6.92 h, respectively, indicating that the change in fog duration induced by ACI (A3DE0 - A0), ARI (A3 - A3DE0), and AE (A3 - A0) is 85, 24, and 109 min, respectively (Figure S4). Despite the significant ARI effect under the extremely polluted condition ($\alpha = 0.05$), the time increase led by ACI is still overwhelming, which is about 3 times more than that of ARI. Although this is just a case study of a few fog events, the results suggest that ACI could outweigh ARI in fog events under different moisture and pollution conditions in general (Figure 2, Table S4, and Figure S4).

5. Conclusion and Implications

Previous studies demonstrate that the long-term fog frequency has been decreasing in East China. This study further reveals that aerosols significantly increase fog duration in East China with 50-year manually recorded fog data. Furthermore, the contributions of ARI and ACI effects are quantitatively studied with WRF-Chem simulations of an extreme fog event (December 31, 2016 to January 4, 2017).

It is found that the control experiment well reproduces this fog event. Sensitive experiments show that ACI significantly increases LWC and fog area and also increases fog duration by 66 min, while ARI increases fog duration by 3 min only. ARI and ACI play different roles in fog spatial distributions during formation, development, and dissipation stages. During the formation stage, ACI advances fog formation, while ARI effect is insignificant. During the development stage, ACI significantly increases fog droplet concentration, decreases droplet radius, and inhibits sedimentation that favors the maintenance of fog. During the dissipation stage, increasing aerosols yield larger COD and AOD. The increase in COD is approximately 1 order of magnitude higher than that in AOD, so ACI blocks more solar radiation than ARI and remarkably delays fog dissipation. Further experiments support that ACI effect could also outweigh ARI effect under extremely polluted conditions.

The aerosol impact on fog lifetime has not been intensively studied before. We find the long-term observational evidence of aerosols promoting fog duration and demonstrate the mechanisms of ARI and ACI effects on fog lifetime with numerical simulations. In this case study, ACI seems to be the dominant influencing factor on fog, and ARI has a minor effect. Therefore, we suggest paying more attention to ACI-related physical processes when studying aerosol–fog interactions. We also suggest applying more stringent emission control to all types of aerosols in order to reduce the hazards of fog and improve air quality. In the future, more numerical simulations are needed to study the observed trend of fog lifetime in different seasons and under different weather systems.

Data Availability Statement

The numerical calculations in this paper have been done on the supercomputing system in the Supercomputing Center of Nanjing University of Information Science & Technology. The ECMWF reanalysis data are obtained from https://apps.ecmwf.int/datasets/data/interim-full-daily/levtype=sfc/. The PM2.5 observational data are downloaded from https://www.aqistudy.cn/. The fog observational data are released on https://github.com/jstzysq/GRLdata. The MEIC inventory is from http://www.meicmodel.org/. The WRF-Chem model is available on https://github.com/NCAR/WRFV3.

Acknowledgments

This work is supported by the National Key Research and Development Program (2016YFA0602003), National Natural Science Foundation of China (42021004, 91544229, 41575148, 41605091, and 41875171), and Postgraduate Research and Practice Innovation of Jiangsu Province Program (KYCX20_0925).

References

Albrecht, B. A. (1989). Aerosols, cloud microphysics, and fractional cloudiness. *Science*, *245*(4923), 1227–1230. https://doi.org/10.1126/science.245.4923.1227

Bond, T. C., Doherty, S. J., Fahey, D. W., Forster, P. M., Berntsen, T., DeAngelo, B. J., et al. (2013). Bounding the role of black carbon in the climate system: A scientific assessment. *Journal of Geophysical Research: Atmospheres*, *118*, 5380–5552. https://doi.org/10.1002/jgrd.50171

Borge, R., Alexandrov, V., Vas, J. J. D., Lumbreras, J., & Rodriguez, E. (2008). A comprehensive sensitivity analysis of the WRF model for air quality applications over the Iberian peninsula. *Atmospheric Environment*, *42*(37), 8560–8574. https://doi.org/10.1016/j.atmosenv.2008.08.032

Bott, A. (1991). On the influence of the physico-chemical properties of aerosols on the life cycle of radiation fogs. *Journal of Aerosol Science*, *21*(1–2), 1–31. https://doi.org/10.1007/BF00119960

Chapman, E. G., Gustafson, W. I., Easter, R. C., Barnard, J. C., Ghan, S. J., Pekour, M. S., & Fast, J. D. (2009). Coupling aerosol–cloud-radiative processes in the WRF-Chem model: Investigating the radiative impact of elevated point sources. *Atmospheric Chemistry and Physics*, *9*(3), 945–964. https://doi.org/10.5194/acp-9-945-2009

Chen, Y. C., Christensen, M. W., Xue, L., Sorooshian, A., Stephens, G. L., Rasmussen, R. M., & Seinfeld, J. H. (2012). Occurrence of lower cloud albedo in ship tracks. *Atmospheric Chemistry and Physics*, *12*(17), 8223–8235. https://doi.org/10.5194/acp-12-8223-2012

Deng, X., Shi, C., Wu, B., Zhang, H., Yang, G., & Yu, C. (2015). Analysis of fog climatic characteristics in Anhui Province during 1970–2009 (in Chinese). *Resources and Environment in the Yangtze Basin*, *24*(12), 2125–2134.

Ding, A. J., Fu, C. B., Yang, X. Q., Sun, J. N., Petaja, T., Kerminen, V. M., et al. (2013). Intense atmospheric pollution modifies weather: A case of mixed biomass burning with fossil fuel combustion pollution in eastern China. *Atmospheric Chemistry and Physics*, *13*(20), 10545–10554. https://doi.org/10.5194/acp-13-10545-2013

Ding, A. J., Huang, X., Nie, W., Sun, J. N., Kerminen, V. M., Petäjä, T., et al. (2016). Enhanced haze pollution by black carbon in megacities in China. *Geophysical Research Letters*, *43*, 2873–2879. https://doi.org/10.1002/2016gl067745

Ding, Y., & Liu, Y. (2014). Analysis of long-term variations of fog and haze in China in recent 50 years and their relations with atmospheric humidity. *Science China Earth Sciences*, *57*(1), 36–46. https://doi.org/10.1007/s11430-013-4792-1

Fan, J., Rosenfeld, D., Yang, Y., Zhao, C., Leung, L. R., & Li, Z. (2015). Substantial contribution of anthropogenic air pollution to catastrophic floods in Southwest China. *Geophysical Research Letters*, *42*, 6066–6075. https://doi.org/10.1002/2015GL064479

Fan, J., Wang, Y., Rosenfeld, D., & Liu, X. (2016). Review of aerosol–cloud interactions: Mechanisms, significance, and challenges. *Journal of the Atmospheric Sciences*, *73*(11), 4221–4252. https://doi.org/10.1175/JAS-D-16-0037.1

Fast, J. D., Gustafson, W. I., Easter, R. C., Zaveri, R. A., Barnard, J. C., Chapman, E. G., et al. (2006). Evolution of ozone, particulates, and aerosol direct radiative forcing in the vicinity of Houston using a fully coupled meteorology–chemistry–aerosol model. *Journal of Geophysical Research*, *111*, D21305. https://doi.org/10.1029/2005JD006721

Fu, G. Q., Xu, W. Y., Yang, R. F., Li, J. B., & Zhao, C. S. (2014). The distribution and trends of fog and haze in the North China Plain over the past 30 years. *Atmospheric Chemistry and Physics*, *14*(21), 11949–11958. https://doi.org/10.5194/acp-14-11949-2014

Gao, J., Zhu, B., Xiao, H., Kang, H., Hou, X., Yin, Y., et al. (2017). Diurnal variations and source apportionment of ozone at the summit of mount Huang, a rural site in Eastern China. *Environmental Pollution*, *222*, 513–522. https://doi.org/10.1016/j.envpol.2016.11.031

Gao, Y., Zhang, M., Liu, Z., Wang, L., Wang, P., Xia, X., et al. (2015). Modeling the feedback between aerosol and meteorological variables in the atmospheric boundary layer during a severe fog–haze event over the North China Plain. *Atmospheric Chemistry and Physics*, *15*(8), 4279–4295. https://doi.org/10.5194/acp-15-4279-2015

Gu, Y., Liou, K. N., Jiang, J. H., Fu, R., Lu, S., & Xue, Y. (2017). A GCM investigation of impact of aerosols on the precipitation in Amazon during the dry to wet transition. *Climate Dynamics*, *48*(7), 2393–2404. https://doi.org/10.1007/s00382-016-3211-7

Gu, Y., Liou, K. N., Xue, Y., Mechoso, C. R., Li, W., & Luo, Y. (2006). Climatic effects of different aerosol types in china simulated by the UCLA general circulation model. *Journal of Geophysical Research*, *111*, D15201. https://doi.org/10.1029/2005JD006312

Guo, J., Su, T., Chen, D., Wang, J., Li, Z., Lv, Y., et al. (2019). Declining summertime local-scale precipitation frequency over China and the United States, 1981–2012: The disparate roles of aerosols. *Geophysical Research Letters*, *46*, 13281–13289. https://doi.org/10.1029/2019GL085442

Guo, T., Zhu, B., Kang, Z., Gui, H., & Kang, H. (2016). Spatial and temporal distribution characteristic of fog days and haze days from 1960–2012 and impact factors over the Yangtze River Delta Region (in Chinese). *China Environmental Science*, *36*(4), 961–969. https://doi.org/10.3969/j.issn.1000-6923.2016.04.001

Huang, X., Ding, A., Wang, Z., Ding, K., Gao, J., Chai, F., & Fu, C. (2020). Amplified transboundary transport of haze by aerosol–boundary layer interaction in China. *Nature Geoscience*, *13*(6), 428–434. https://doi.org/10.1038/s41561-020-0583-4

IPCC. (2013). *Climate change 2013: The physical science basis*. Contribution of working Group I to the Fifth Assessment Report of the Intergovernmental Panel on Climate Change. Cambridge, UK/New York, NY: Cambridge University Press. https://doi.org/10.1017/CBO9781107415324

Jia, X., Quan, J., Zheng, Z., Liu, X., Liu, Q., He, H., & Liu, Y. (2018). Impacts of anthropogenic aerosols on fog in North China Plain. *Journal of Geophysical Research: Atmospheres*, *124*, 252–265. https://doi.org/10.1029/2018jd029437

Jiang, Q., Yin, Y., Shan, Y., Li, A., & Chen, Q. (2014). The effect of artificial aerosols on orographic precipitation: A case study over the Yellow Mountain (in Chinese). *Transactions of Atmospheric Sciences*, *37*(04), 405–413. https://doi.org/10.13878/j.cnki.dqkxxb.20121105001

Koren, I., Martins, J. V., Remer, L. A., & Afargan, H. (2008). Smoke invigoration versus inhibition of clouds over the Amazon. *Science*, *321*(5891), 946–949. https://doi.org/10.1126/science.1159185

Kunkel, B. A. (1984). Parameterization of droplet terminal velocity and extinction coefficient in fog models. *Journal of Applied Meteorology*, *23*(1), 34–41. https://doi.org/10.1175/1520-0450(1984)023<0034:PODTVA>2.0.CO;2

Li, M., Zhang, Q., Streets, D. G., He, K. B., Cheng, Y. F., Emmons, L. K., et al. (2014). Mapping Asian anthropogenic emissions of non-methane volatile organic compounds to multiple chemical mechanisms. *Atmospheric Chemistry and Physics*, *14*(11), 5617–5638. https://doi.org/10.5194/acp-14-5617-2014

Li, Y., Cao, L., Gao, S., & Luo, B. (2010). The current stage and development of MICAPS (in Chinese). *Meteorological Monthly*, *36*, 50–55.

Li, Z., Guo, J., Ding, A., Liao, H., Liu, J., Sun, Y., et al. (2017). Aerosol and boundary-layer interactions and impact on air quality. *National Science Review*, *4*(6), 810–833. https://doi.org/10.1093/nsr/nwx117

Li, Z., Lau, W. K. M., Ramanathan, V., Wu, G., Ding, Y., Manoj, M. G., et al. (2016). Aerosol and monsoon climate interactions over Asia. *Reviews of Geophysics*, *54*, 866–929. https://doi.org/10.1002/2015RG000500

Li, Z., Niu, F., Fan, J., Liu, Y., Rosenfeld, D., & Ding, Y. (2011). Long-term impacts of aerosols on the vertical development of clouds and precipitation. *Nature Geoscience*, *4*(12), 888–894. https://doi.org/10.1038/ngeo1313

Li, Z., Wang, Y., Guo, J., Zhao, C., Cribb, M. C., Dong, X., et al. (2019). East Asian Study of Tropospheric Aerosols and their Impact on Regional Clouds, Precipitation, and Climate (EAST-AIR CPC). *Journal of Geophysical Research: Atmospheres*, *124*, 13026–13054. https://doi.org/10.1029/2019JD030758

Li, Z., Xia, X., Cribb, M., Mi, W., Holben, B., Wang, P., et al. (2007). Aerosol optical properties and their radiative effects in northern China. *Journal of Geophysical Research*, *112*, D22S01. https://doi.org/10.1029/2006JD007382

Maalick, Z., Kühn, T., Korhonen, H., Kokkola, H., Laaksonen, A., & Romakkaniemi, S. (2016). Effect of aerosol concentration and absorbing aerosol on the radiation fog life cycle. *Atmospheric Environment*, *133*, 26–33. https://doi.org/10.1016/j.atmosenv.2016.03.018

Niu, F., Li, Z., Li, C., Lee, K., & Wang, M. (2010). Increase of wintertime fog in China: Potential impacts of weakening of the Eastern Asian monsoon circulation and increasing aerosol loading. *Journal of Geophysical Research*, *115*, D00K20. https://doi.org/10.1029/2009JD013484

Rosenfeld, D., Lohmann, U., Raga, G. B., O'Dowd, C. D., Kulmala, M., Fuzzi, S., et al. (2008). Flood or drought: How do aerosols affect precipitation? *Science*, *321*(5894), 1309–1313. https://doi.org/10.1126/science.1160606

Shi, C., Yang, J., Qiu, M., Xie, W., & Zhang, H. (2008). Impacts of urban development on long-term variation of fog (in Chinese). *Climatic and Environmental Research*, *13*(3), 327–336.

Stolaki, S., Haeffelin, M., Lac, C., Dupont, J. C., Elias, T., & Masson, V. (2015). Influence of aerosols on the life cycle of a radiation fog event. A numerical and observational study. *Atmospheric Research*, *151*, 146–161. https://doi.org/10.1016/j.atmosres.2014.04.013

Tie, X., Huang, R., Cao, J., Zhang, Q., Cheng, Y., Su, H., et al. (2017). Severe pollution in China amplified by atmospheric moisture. *Scientific Reports*, *7*, 15760. https://doi.org/10.1038/s41598-017-15909-1

Twomey, S. A. (1977). The influence of pollution on the shortwave albedo of clouds. *Journal of the Atmospheric Sciences*, *34*(7), 1149–1154. https://doi.org/10.1175/1520-0469(1977)034<1149:TIOPOT>2.0.CO;2

Wu, G., Li, Z., Fu, C., Zhang, X., Zhang, R., Zhang, R., et al. (2016). Advances in studying interactions between aerosols and monsoon in China. *Science China Earth Sciences*, *59*(1), 1–16. https://doi.org/10.1007/s11430-015-5198-z

Yan, S., Zhu, B., Huang, Y., Zhu, J., Kang, H., Lu, C., & Zhu, T. (2020). To what extents do urbanization and air pollution affect fog? *Atmospheric Chemistry and Physics*, *20*(9), 5559–5572. https://doi.org/10.5194/acp-20-5559-2020

Yan, S., Zhu, B., & Kang, H. (2019). Long-term fog variation and its impact factors over polluted regions of East China. *Journal of Geophysical Research: Atmospheres*, *124*, 1741–1754. https://doi.org/10.1029/2018JD029389

Zhang, J., Ye, C., & Mo, R. (2017). Comparison analysis of variability of meteorological elements observed at three mountain observatories over Central-Eastern China (in Chinese). *Plateau Meteorology*, *36*(01), 107–118. https://doi.org/10.7522/j.issn.1000-0534.2015.00103

Zhang, N., & Ma, X. (2017). Analysis of the June 2018 atmospheric circulation and weather (in Chinese). *Meteorological Monthly*, *43*(4), 508–512. https://doi.org/10.7519/j.issn.1000-0526.2017.04.014

Zhong, S., Qian, Y., Zhao, C., Leung, R., & Yang, X. (2015). A case study of urbanization impact on summer precipitation in the Greater Beijing Metropolitan Area: Urban heat island versus aerosol effects. *Journal of Geophysical Research: Atmospheres*, *120*, 10903–10914. https://doi.org/10.1002/2015JD023753

Zhou, B., & Du, J. (2010). Fog prediction from a multimodel mesoscale ensemble prediction system. *Weather and Forecasting*, *25*(1), 303–322. https://doi.org/10.1175/2009WAF2222289.1

Zhu, B., & Guo, T. (2016). Review of the impact of air pollution on fog (in Chinese). *Advances in Meteorological Science and Technology*, *6*(2), 56–63.

Reference From the Supporting Information

Abdul-Razzak, H., & Ghan, S. J. (2002). A parameterization of aerosol activation 3. Sectional representation. *Journal of Geophysical Research*, *107*(D3), 4026. https://doi.org/10.1029/2001JD000483